THE STRING MODEL OF DISLOCATION DAMPING REVISITED*

F. MARCHESONI[a,b] AND D. SEGOLONI[a]

[a]Istituto Nazionale di Fisica Nucleare, Universita' di Perugia
I-06100 Perugia, Italy

[b]Dipartimento di Matematica e Fisica, Universita' di Camerino
I-62032 Camerino, Italy

(Received February 15, 1993)

The classic Granato-Lücke model for dislocation damping is revisited by accounting for possible refinements to the basic vibrating string mechanism. We argue that the perturbation approach, which consists in separating the (linear) dislocation dynamics from the equilibrium lattice environment, is not suitable, no matter how accurate the description of the coupling, to explain the finite decrement function observed experimentally in a variety of samples at vanishingly small frequencies. A few ideas for a more general theory are discussed in some detail.

PACS numbers: 61.72. Bb

1. Introduction

The attenuation of sound waves in crystals was the subject of a tremendous amount of both experimental and theoretical work in the 50's and early 60's [1, 2]. As the military industry focus shifted towards microelectronics, the interest for physical acoustics seemed to fade away. A surge of fresh curiosity has been reported recently in the literature concerned with the problem of extremely accurate mechanical measurements [3, 4]. In particular, the approval of two big experiments for the interferometric detection of gravitational waves (the American project LIGO and the French–Italian collaboration VIRGO) stimulated new investigations on the role of internal friction crystals. As a matter of fact, the purpose of the above experiments

* Presented at the V Symposium on Statistical Physics, Zakopane, Poland, September 21–30, 1992.

boils down to measuring of the response of a forced mechanical pendulum (the single mirrors suspended in the interferometric cavity), where the major source of uncertainty comes from the internal (or thermal) noise in the suspension device (typically, wires made of metallic alloys or fused quartz).

The motion of a defect known as a *dislocation* provides a very efficient mechanism of dissipation of mechanical energy in lattice structures [7, 8] under the operating conditions of both LIGO and VIRGO gravitational antennas. The first experimental evidence of the role of dislocations as a source of internal friction in crystals was produced back in the early 40's [9, 10] by studying the dependence of the decrement function Δ of a sample (defined as the ratio of the energy lost per cycle to half the maximum stored energy) on the orientation of the crystallographic axes [9], the impurity density [7], and small plastic deformations in the elastic stress-strain regime [10].

In spite of the very many parameters required for an exhaustive explanation of the phenomenon of dislocation damping, most experimental observations may be interpreted, at least qualitatively, in terms of a very simple model: *the vibrating string model.* Such a model was fully developed by Granato and Lücke (GL model [7, 11]) and is outlined in the forthcoming Section. In Sections 3–7 we present a number of refinements of the basic dissipation mechanism and estimate the relevant corrections to the earliest predictions of the GL model. In particular, we discuss the choice of a suitable impurity distribution (Section 3), the effects of the impurity diffusion (Section 4) and finite temperature (Section 5), the limit of weak dislocation–impurity interaction (Section 6) and the role of lattice interactions (Section 7). We conclude our analysis in Section 8 pointing out that the GL model is very unlikely to explain the finite values of the decrement function at vanishingly small acoustic frequencies observed experimentally for a variety of samples over the last three decades [4, 5, 8, 12]. Finally, we suggest that a stick-and-slip mechanism of dislocation diffusion may be more appropriate to interpret the experiments on crystal internal friction at low frequencies.

2. The Granato–Lücke model

A great many people contributed to the development of the so-called GL model. For a historical presentation the reader is referred to Granato and Lücke review paper [7]. In order to appreciate the basic mechanism of such a model, it is necessary to know only little of dislocation theory [2]. A dislocation line is a linear imperfection in a lattice structure. At its center line (assimilated here to a string) the lattice is strongly disturbed, whereas at distances much larger than the lattice spacing(s) the disturbance

is described by an elastic stress field, that is a permanent shear deformation or slip step at infinite distance. The type of dislocations, of interest for the present analysis, are able to glide along certain crystallographic planes (slip planes) under the action of an applied stress. The magnitude and direction of the slip step is characterized by the Burgers vector b of the dislocation. Thus, if a dislocation segment of length l moves a distance ξ, its inelastic contribution to the strain ε_D is given by $bl\xi$. An external shear stress with perpendicular component σ in the dislocation slip plane, exerts a force $b\sigma$ on a dislocation of length unity. The possibility for the dislocation to move in the presence of an external stress diminishes the sample elastic constant. The resistive forces which oppose the free motion of dislocations in a crystal are responsible for the mechanical energy losses known as dislocation damping. The relevant decrement function is defined in terms of σ and ε_D as $\Delta = G\frac{\int \sigma d\varepsilon_D}{\int \sigma d\sigma}$.

In a real crystal glissile dislocations break up to form a network of dislocation segments (or loops) with a characteristic length L_N in the range $[10^{-4} - 10^{-3}]$ cm or wider, depending on the material and preparation of the sample [1]. It is usually assumed that the loops are tightly pinned at the network nodes [2]. Defects such as impurities, vacancies and interstitials, have a lower energy near the core of a dislocation than in the good lattice and, therefore, act as pinning-points on the network loops. Moreover, at finite temperature defects like impurities are free to diffuse and, as a consequence of their interaction with the dislocation line, their linear concentration c on the loops attains a higher equilibrium value than the average lattice concentration c_0, *i.e.*

$$c = c_0 \exp\left(\frac{|E_C|}{kT}\right), \tag{2.1}$$

where E_C is the *negative* impurity–dislocation interaction energy introduced by Cottrell [1, 2].

Under stress the network loops bow out like an *elastic* string, being held back at the pinning-points (Fig. 1). The energy of a bowed out loop is greater than that of a straight loop pinned by the same pair of *fixed* impurities, due to the fact that its length is greater. Such an effective loop tension provides the restoring mechanism in the vibrating string model for dislocations. If the applied stress is large enough, the force exerted on the loops at the pins can be thus strong as to overcome the Cottrell binding force and the so-called depinning (or breakaway) process sets in.

It is apparent that the loss is made up of two different contributions. The *first type* of loss is due to the frictional force acting upon the moving dislocation loop as a result of its interaction with the lattice environment. The physical sources of such a drag force are discussed briefly in Section 8.

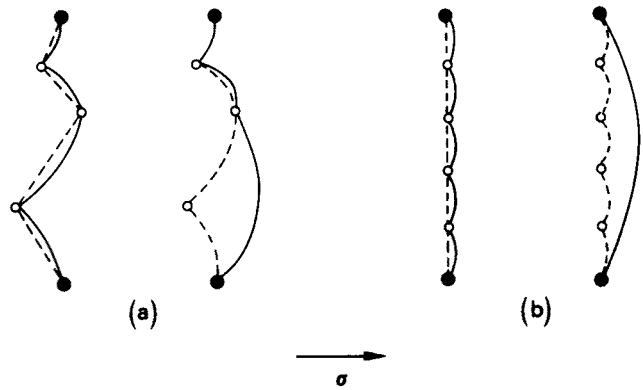

Fig. 1. Examples of pinned network loop. Solid dots: the network nodes at the end-points, circles: pinning-points randomly (a) and equally spaced (b); solid and dashed curves represent the dislocation loop under increasing stress.

The vibrating string takes on a phase-lag with respect to a weak oscillating external stress. The resulting dynamic loss is frequency dependent, since the underlying dissipative mechanism is a resonant one. The *second type* of loss is due to the depinning of dislocation segments connecting adjoint defects, say impurities, in the presence of a stronger oscillating stress (Fig.1(b)). During the unloading part of the stress cycle, the network loop segments get pinned down again, possibly back into the initial relaxed configuration, but following a different path and, thus, giving rise to a hysteresis cycle. The resulting loss is proportional to the area encircled by the stress-dislocation strain cycle (σ, ε_D). Since for a given stress amplitude such a hysteresis cycle is mostly a microscopic property of the individual sample, this type of loss is expected to be frequency independent.

2.1. The dislocation resonance loss

A single pinned-down dislocation loop obeys the following partial differential equation for an elastic string [7]

$$A\frac{\partial^2 \xi}{\partial t^2} + B\frac{\partial \xi}{\partial t} - C\frac{\partial^2 \xi}{\partial y^2} = b\sigma(t)\,, \tag{2.2a}$$

where $\xi = \xi(y, t)$ and the boundary conditions are $\xi(0, t) = \xi(l, t) = 0$. Here y denotes the coordinate of an element of a dislocation line of length l at rest on the positive y-semi axis and ξ is its displacement in the direction of an applied perpendicular stress $\sigma = \sigma(x, t)$. The parameters A, B and C are the effective string mass, the viscous (or drag) force and the effective tension per unit of dislocation length, respectively. In GL calculations

the random force attached to the drag force by the fluctuation–dissipation theorem, is neglected relative to the oscillating bias generated by the external stress without loss of generality. The stress wave travelling through a crystal embedding a dislocation network obeys a further partial differential equation [7]

$$\frac{\partial^2 \sigma}{\partial x^2} - \frac{\rho}{G}\frac{\partial^2 \sigma}{\partial t^2} = \Lambda \rho b \frac{\partial^2}{\partial t^2}\bar{\xi}(l,t)\,, \tag{2.2b}$$

where ρ is the density of the material, G the shear modulus and Λ the total length of dislocation line per unit of volume. The average loop displacement $\bar{\xi}$ is defined as $(1/l)\int_0^l \xi(y,t)dy$.

The decrement function $\Delta_R(\omega)$, corresponding to the dynamic loss in the vibrating string model (2.2), has been calculated explicitly by Granato and Lücke [11] for an arbitrary travelling stress wave $\sigma(x, t)$. However, on choosing $\sigma(x, t) = \sigma_0 \cos\omega t$, the resonance contribution of $\Delta(\omega)$ can be cast in the more tractable form:

$$\Delta_R(\omega) = \Omega \Lambda b G \frac{\int_0^{2\pi/\omega} \bar{\xi}(l,t)\sigma_0 \sin\omega t dt}{\int_0^{2\pi/\omega} \sigma_0^2 \cos^2\omega t dt}\,. \tag{2.3}$$

Solving Eq. (2.2a) for the fundamental string mode and making use of definition (2.3), one obtains the approximate solution

$$\frac{\Delta_R(\omega)}{\Delta_0} = \Omega \Lambda l^2 \frac{\frac{d}{\omega_0}\frac{\omega}{\omega_0}}{\left[1-\left(\frac{\omega}{\omega_0}\right)^2\right]^2 + \left(\frac{d}{\omega_0}\right)^2\left(\frac{\omega}{\omega_0}\right)^2}\,, \tag{2.4}$$

where

$$\Delta_0 = \frac{8Gb^2}{\pi^3 C}\,, \quad d = \frac{B}{A}\,, \quad \omega_0 = \frac{\pi}{l}\left(\frac{C}{A}\right)^{1/2}$$

Ω is an orientation ratio (the square of the resolved shear stress in the slip plane to the square of the applied stress) and the subscript R denotes the resonance loss

The experimental consequences of Eq. (2.4) are discussed in detail in Ref. [7]. Here, we limit ourselves to remember that for most high-purity metals at not too low temperature $\frac{d}{\omega_0} \gg 1$, *i.e.* the string dynamics (2.2) is overdamped and Eq. (2.4) may be simplified as

$$\frac{\Delta_R(\omega)}{\Delta_0} = \Omega \Lambda l^2 \frac{\omega\tau}{1+(\omega\tau)^2}\,, \tag{2.5}$$

where $\tau = \frac{d}{\omega_0^2} = \frac{Bl^2}{\pi^2 C}$. The temperature dependence of the relaxation time τ is due mainly to the power-like temperature dependence of B (see

Section 8). Therefore, no activation mechanism is involved in the process. Most notably, $\Delta_R(\omega)$ is independent of the stress amplitude and tends to zero for both $\omega \to 0$ and $\omega \to \infty$. As anticipated in the Introduction, the prediction $\Delta_R(0) = 0$ is contradicted by the experimental evidence.

2.2. The dislocation breakaway loss

Breakaway of dislocations from a pinning-point occurs when the force applied on a dislocation segment just exceeds that exerted on the segment by the pinning-point itself. For the adjacent loops of length l_1 and l_2 in Fig. 1(b), the former force is given by $b\sigma(l_1 + l_2)/2$, whereas the pinning force at zero temperature can be estimated in terms of the Cottrell energy E_C, *i.e.* $|E_C|/b$. Therefore, the breakaway stress σ_b is given locally by the condition $b\sigma_b(l_1+l_2)/2 = |E_C|/b$ (*single-pin approximation*). In most cases, this value for σ_b is much smaller than the value estimated by Frank and Read [2] for the breakaway stress σ_F from a network node $\sigma_b \ll \sigma_F = Gb/L_N$. It follows that the longest pair of pinned loops in a network segment are likely to breakaway first, thus causing the remaining loops to unpin. This is certainly the case if the pins lie on a straight segment connecting the relevant network nodes. However, different network loops have different length and pinning-point distribution and, consequently, different breakaway stresses [13, 14].

To calculate the amplitude dependence of the decrement function, Granato and Lücke introduced the following simplifying assumptions about the equilibrium distribution function $N(l)$ of the loop length l: *(i)* all of the network loop length L_N are the same size; *(ii)* $L_N \gg L_P$ where L_P is the average value of the loop length l; l is distributed according to the maximally uncorrelated distribution compatible with the model, *i.e.* an exponential distribution [15] (see Section 3). Under these assumptions the decrement function at zero forcing frequency reads [7, 11]:

$$\frac{\Delta_B(0)}{\Delta_0} = \frac{\Omega L_N \Lambda_B}{\pi L_P} \frac{\sigma_B}{\sigma_0} \exp\left(-\frac{\sigma_B}{\sigma_0}\right), \tag{2.6}$$

where σ_0 is the stress amplitude, σ_B is the average breakaway stress and the subscript B denotes the breakaway loss. In particular, Λ_B denotes the total length of the dislocation line per unit of volume involved in the breakaway process. The strain amplitude dependence ($\varepsilon = \sigma/G$) predicted in Eq. (2.6) is in generally good agreement with the experimental observations at *finite* temperature.

In the vibrating string model, the dynamics and the very nature of dislocations are highly idealized leaving the reader with the task of introducing the refinements needed to fully interpret the results of measurements carried

out on real samples. For instance, the energy of a dislocation is distributed over a cylinder with radius of the order b and, therefore, interactions between adjacent loops may become appreciable [16], the line tension depends upon the type of dislocation and may be affected by anisotropy [17]. Although such effects could not be estimated quantitatively, it is believed [18] that they can be averaged out by rescaling suitably the model parameters. Fortunately, a number of more conspicuous effects can be treated analytically as shown in the forthcoming Section with particular attention to the problem of the residual resonance loss at zero frequency.

3. The loop distribution function

Since the earliest formulations of the dislocation string model it was understood that the appropriate choice for the loop-length distribution $N(l)$ is a crucial ingredient to achieve a favourable agreement with the experimental measurements [15]. For instance, the resonant peak of $\Delta_R(\omega)$ for a single vibrating dislocation loop (2.4)–(2.5) is too narrow when compared with the measurements of the decrement function in the MHz-range. On the other hand, the exponential expression for $N(l)$ introduced by Granato and Lücke to determine $\Delta_B(0)$, Eq. (2.6), was justified by neglecting the pinning-point dynamics. In the present Section we derive a more general expression for $N(l)$ based on equilibrium thermodynamics. We remark that at the basis of the GL model is the factorization of the dislocation dynamics from the lattice dynamics, which is made up mainly of vibrational modes (phonons) and defect diffusion. Whithin such an approach, which is ultimately questioned in the conclusions of the present paper, a few specific assumptions may be introduced safely. Due to the interactions with the dislocation line, impurities migrate through lattice structure to form a "Cottrell atmosphere" (2.1) around the network segments. At zero temperature a dislocation network segment is pinned down by impurities and no thermal depinning is to be considered (see Section 5). At thermal equilibrium and in the absence of external stresses, it is conceivable that the impurities are arranged like in Fig. 1(a), rather than like in Fig. 1(b). The dislocation tension drags the pinning-points of the network loop close to the straight segment connecting the network nodes. The impurities are relatively free to diffuse along a vibrating dislocation line, whereas the transverse movement is suppressed by lattice interactions (*i.e.* it takes place on too long a time scale). A network loop of length L_N is thus modellized as in Fig. 2: a vibrating elastic string pinned at its end-points A and B and passing through a number of small rings free to glide along the segment AB of length L_N (the movable pinning-points) subject to viscous friction.

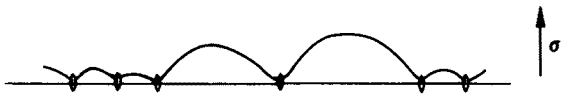

Fig. 2. Example of dislocation loop pinned down by diffusing impurities.

In the presence of a constant external stress σ the distribution function $N(l,\sigma)$ is obtained by minimizing the total free energy $F(\sigma)$ of the system string+pinning-points under the following constraints:

$$\int_0^{L_N} N(l,\sigma)dl = 1\,, \tag{3.1}$$

and

$$\int_0^{L_N} lN(l,\sigma)dl = L_P\,. \tag{3.2}$$

The average dislocation loop length at $\sigma = 0$ is $L_P = L_N/N$, by definition. The total free energy has been calculated, under the assumptions spelled above, by Bauer [19] and Alefeld [20]:

$$F(\sigma) = NkT \int_0^{L_N} N(l,\sigma)[\ln N(l,\sigma) + \frac{\alpha}{a}l - \beta\sigma^2 l^3]dl \tag{3.3}$$

apart from an irrelevant additive constant. The meaning of the parameters a, α and β is illustrated now in some detail.

The quantity $F(\sigma)$ is made up of three distinct contributions:

(1) *configurational free energy*: the first term is the free energy related to the distribution of the $N-1$ pinning-points along the network segment discretized in unit cells with length a (typically the relevant lattice spacing). This is a purely configurational term, where the string dynamics and the external stress σ play no role. When used to calculate $N(l,\sigma)$, such a free energy term yields the σ-independent expression [15]

$$N(l) = \frac{1}{L_P}\exp\left(-\frac{l}{L_P}\right) \tag{3.4}$$

employed in Section 2.2.

(2) *vibrational free energy*: the second term accounts for the vibrational modes of the pinning dislocation–network loop. On neglecting lattice

interactions (whose treatment is postponed to Section 7) and assuming the condition of *strong pinning* (when ignoring thermal depinning, dislocation breakaway can only take place when locally $\sigma \geq \sigma_B$), the calculation of the *classical* vibrational free energy term is straightforward [19]. The parameter α is a function of a Debye characteristic temperature Θ_D of the dislocation line $\alpha = \Theta_D/4T + \ln(\Theta_D/T) - 1$. Most notably, one can verify that the classical internal energy per unit of length of a vibrating dislocation line in the absence of applied stress is exactly kT, as expected. It follows that the internal (or thermal) stress due to the string vibrations gives rise to no net force on the pinning points parallel to the dislocation line. Furthermore, the loop length distribution function (3.4) is left unchanged when including the vibrational free energy term.

(3) *stress dependent free energy*: as shown by the third free energy term, coupling the dislocation line with an external stress σ affects the loop length distribution appreciably even for values of σ less than σ_B. The potential energy of an elastic string in the presence of a constant stress σ can be easily calculated under the simplifying assumptions introduced above [19]. The string straight line is deformed into an arc of parabola, whose potential energy, $-\beta\sigma^2 l^3$ with $\beta = b^2/24CkT$, appears in the corresponding free energy term of Eq. (3.3). From the stress dependent term of the potential energy one derives an expression for the force acting on the n-th pinning-point parallel to the dislocation line

$$F_n = \frac{(b\sigma)^2}{8C}(l_n^2 - l_{n+1}^2)\,. \tag{3.5}$$

As a consequence of impurity diffusion, the shorter loops tend to get shorter and *vice versa*.

The latter statement is confirmed by the explicit calculation of $N(l,\sigma)$. Minimized $F(\sigma)$ (3.3) with the constraints (3.1) and (3.2) yields [21]:

$$N(l,\sigma) = \begin{cases} \frac{1}{L_P}\exp\left(-\frac{l}{L_P}\right) & (\sigma < \sigma_C) \\ \frac{1}{L_\sigma}\left(2\frac{L_P - L_\sigma}{L_P}\right)^{l/L_N} \exp\left[-\frac{l}{L_\sigma}\left(1 - \left(\frac{l}{L_N}\right)^2\right)\right] & (\sigma \geq \sigma_C)\,, \end{cases} \tag{3.6}$$

where $L_\sigma = (\beta\sigma^2 L_N^2)^{-1}$ and $\sigma_C = (N/\beta L_N^3)^{1/2}$. As expected, when σ_C is exceeded and $\sigma_C \ll \sigma_B$, most of the N loops are compressed by a few loops that grow to large dimensions. It is understood that for the fraction of the dislocation network loops for which $\sigma \geq \sigma_B$ the above distribution collapses to [11]

$$N(l,\sigma) = 2\delta(l - L_N)\,. \tag{3.7}$$

The pinning-point diffusion makes the transition from the exponential distribution (3.4) to the entirely depinned configuration (3.7) smoother than anticipated in Section 2.1.

We make now a few important remarks:

(i) the single vibrating-string prediction for the decrement function $\Delta_R(\omega)$ in Eqs (2.4)–(2.5) should be averaged over the loop length distribution (3.6),

$$\Delta_R(\omega) \to \bar{\Delta}_R(\omega) = \int_0^{L_N} \Delta_R(\omega) N(l, \sigma) dl \,, \tag{3.8}$$

thus obtaining the observed broadening of the resonance peak at around ω_0 [7];

(ii) due to possible entropy variations, a more general expression for the impurity "Cottrell atmosphere" (2.1) is

$$c = c_0 \exp\Big(-\frac{F_C}{kT}\Big) \,, \tag{3.9}$$

where F_C is the free energy contribution $E_C - TS_C$ associated with accommodating one extra impurity on the thermalized dislocation line [19, 20]. Accordingly, $S_C \approx -k + \frac{k}{2} \ln c$ (apart from a negligible additive constant);

(iii) the estimate of Section 2.1. for the mechanical breakaway stress σ_B should be modified, as well. When accounting for impurity diffusion, a simple free-energy argument leads to [19]

$$\sigma_C = \frac{kT}{2|F_C|} \sigma_B \,, \tag{3.10}$$

whence the inequality $\sigma_B > \sigma_C$ for most experimental samples.

4. Pinning-point diffusion

In the foregoing Section we showed that the string-impurity interaction determines a correlation in the loop length distribution at equilibrium. However, impurity diffusion also affects the *relaxation* properties of the string-impurity system, thus making a generalization of the GL calculation of the decrement function necessary. Although such very notion has been around in the literature since the work of Yamafuji and Bauer [21], we introduce here an explicit expression for the diffusion controlled decrement $\Delta_D(\omega)$.

Our starting point is the model for the string-impurity system outlined in Section 3. We keep neglecting lattice interactions and the transverse motion of the pinning-points relative to the dislocation line. As a matter of

fact, at room temperature the rms stress exerted on a dislocation loop length l by the thermalized vibrational modes of the string (thermal stress), is approximated to [19] $\sigma_{\text{th}} \simeq (8kTG/L_P^3)^{1/2}$ and is quite large, $\sigma_{\text{th}} \sim N\sigma_C$. Moreover, the transverse force acting on the n-th pinning-point in the presence of the applied stress σ is [19] $\frac{1}{2}\sigma b(l_n + l_{n+1})$. Experimentally, the applied stress oscillates in time $\sigma(t) = \sigma_0 \cos\omega t$, whereas $\sigma_{\text{th}}(t)$ may be represented as a zero-mean random process. In conclusion, the net transverse force exerted by the vibrating string on a pinning-point vanishes when time averaged on many a forcing cycle. A few exceptional cases where the above assumption is not tenable are quoted, for instance, in Ref. [2] (see p. 78).

The *zero temperature* limit invoked in Section 3 should be taken with some caution. It is generally meant that thermal depinning may be safely neglected ($kT \ll |E_C|$, so that $\sigma_{\text{th}} \ll \sigma_C$), whereas the impurity diffusion coefficient along the dislocation line $D_P = kT/\gamma_P$ is finite (and, in general, much larger than the bulk diffusion coefficient). The relevant frictional drag coefficient γ_P is taken constant at temperatures where the thermal activation energy kT is much larger than the lattice potential barriers (*i.e.* $T \gg \Theta_P$ with Θ_P the Peierls temperature). Of course, corrections to $\Delta_R(\omega)$ due to impurity diffusion are expected at frequencies much lower than the characteristic relaxation time of the loop length distribution function.

The time dependence of $N(l, \sigma)$ is described by the following Fokker–Planck equation [21]

$$\frac{\partial}{\partial t} N(l, \sigma; t) = 2D_P \frac{\partial}{\partial l}\left[-\frac{f(l, \sigma)}{kT} + \frac{\partial}{\partial l}\right] N(l, \sigma; t)\,, \tag{4.1}$$

where the generalized force $f(l, \sigma)$ acting on the pinning-points is derived from the relevant free energy, *i.e.*

$$f(l, \sigma) = \frac{kT}{N(l, \sigma)} \frac{\partial N(l, \sigma)}{\partial l} \tag{4.2}$$

and, by definition, $N(l, \sigma) = \lim_{t \to \infty} N(l, \sigma; t)$ is the equilibrium distribution (3.6). On assuming for simplicity and without loss of generality that $\sigma < \sigma_C$, the diffusion equation (4.1) boils down to

$$\frac{\partial}{\partial t} N(l, \sigma; t) = 2D_P \frac{\partial}{\partial l}\left[\frac{1}{L_P} + \frac{\partial}{\partial l}\right] N(l, \sigma; t)\,. \tag{4.3}$$

The relaxation time of $N(l, \sigma; t)$ follows immediately $\tau = 2L_P^2/D_P$, so that impurity diffusion effects on dislocation damping are expected for $\omega\tau \leq 1$.

Values of τ of the order 1 sec are commonly measured for sound attenuation [20, 21].

The calculation of the diffusion controlled decrement function $\Delta_D(\omega)$ runs parallel to the GL derivation. We remember that in the absence of diffusion l is a constant and definition (2.3) can be rewritten as

$$\Delta_R(\omega) = \frac{\Lambda b G \Omega}{\sigma_0} |\operatorname{Im} \bar{\xi}(l, \omega)|, \tag{4.4}$$

where $\bar{\xi}(l, \omega)$ denotes the relevant Fourier coefficient of $\bar{\xi}(l, t)$. Due to diffusion l becomes a random variable with stationary distribution (3.4). It is then natural to replace $\bar{\xi}(l, t)$ with the two-time quantity

$$\frac{1}{L_P} \int_0^{L_N} l(0) \bar{\xi}(l(t), t) N(l, \sigma) dl. \tag{4.5}$$

On substituting Eqs (3.11) and (4.5) into Eq. (4.4) one obtains

$$\Delta_D(\omega) = \frac{2G\Lambda b\Omega}{\sigma_0 L_P} \int_0^{2\pi/\omega} \langle \bar{\xi}(l(t), t) l(0) \rangle \sin \omega t dt, \tag{4.6}$$

where $\langle \ldots \rangle$ denotes the average in Eq. (4.5) and the subscript D denotes the diffusion controlled loss. The general expression (4.6) can be made more tractable by rewriting $l(t)$ as $L_P + \delta(t)$ and approximating $\bar{\xi}(l(t), t)$ with $\bar{\xi}(L_P, t) + \frac{\partial \bar{\xi}}{\partial l}(L_P, t) \delta l(t)$, whence

$$\Delta_D(\omega) = \bar{\Delta}_R(\omega) + \frac{2G\Lambda b\Omega}{\sigma_0 L_P} \int_0^{2\pi/\omega} \frac{\partial \bar{\xi}}{\partial l}(L_P, t) \langle \delta l(t) \delta l(0) \rangle \sin \omega t dt. \tag{4.7}$$

The Fokker–Planck equation (4.3) can be solved analytically [22]. Standard calculations yield the following asymptotic behaviour for the autocorrelation function of $\delta l(t)$

$$\lim_{t \to \infty} \langle \delta l(t) \delta l(0) \rangle \sim \frac{1}{\sqrt{t}} \exp\left(-\frac{D_P t}{2L_P^2}\right), \tag{4.8}$$

with $\langle \delta l^2 \rangle = L_P^2$. Accordingly, the impurity diffusion contribution to $\Delta_D(\omega)$ has the same dependence as $\Delta_R(\omega)$ for $\omega \to 0$. We are thus led to conclude that the observed residual decrement at zero frequency cannot be explained in terms of a purely diffusive model.

5. Thermal depinning

In this Section we summarize the results of a score of papers [23–25] devoted to the study of a more realistic depinning mechanism. First of all, if we neglect the phenomenon of impurity diffusion, the bare string-impurity interaction potential can be represented by a function $U(\xi)$ (ξ is the string displacement from the relaxed straight-segment configuration) with a *finite* characteristic range r. As pointed out by Cottrell first (for a review see Refs [23] and [24]), $U(\xi)$ has the shape of a smooth potential well with depth U_0 and horizontal asymptote as $y \to \pm\infty$. The actual analytical expression for $U(\xi)$ is immaterial, here. Secondly, depinning takes place due to either an external applied stress of magnitude σ larger than the breakaway value σ_B introduced in Section 2, or *thermal activation* [22]. Indeed, thermal fluctuations may help the dislocation line to overcome the binding potential even in the presence of relatively small stress bias. We formulate here the treatment of Refs [23] and [24] as a *nucleation* mechanism [26, 27].

Let us consider the dislocation network loop of length L_N of Section 2. On including the interaction terms with an impurity distribution $\rho(y)$, but still neglecting lattice interactions, Eq. (2.2) in the overdamped limit ($A = 0$) becomes

$$B\frac{\partial \xi}{\partial t} - C\frac{\partial^2 \xi}{\partial y^2} = b\sigma - \rho(y)\frac{\partial U(\xi)}{\partial \xi} + \eta(y,t)\,. \tag{5.1}$$

Here, contrary to Eq. (2.2), σ is a positive constant and the zero mean, Gaussian, delta correlated spatio-temporal noise $\eta(y,t)$ is included explicitly, $\langle \eta(y,t)\eta(0,0)\rangle = 2BkT\delta(y)\delta(t)$. On further ignoring impurity diffusion, we can assume a uniform pin distribution

$$\rho(y) = \frac{1}{L_P}\,. \tag{5.2}$$

In the continuum limit, implicit in Eq. (5.1), such a choice is equivalent to the equally spaced pin distribution of Fig. 1(b).

For low stress values Eqs (5.1) and (5.2) admit two constant solutions for $\xi(y,t)$. On setting its l.h.s. term equal to zero, Eq. (5.1) admits two solutions for

$$\sigma < \sigma_B = \frac{U_0}{rbL_P}\,. \tag{5.3}$$

For the potential shape $U(\xi)$ described above, one of the two solutions ξ_s ($\xi_s \ll r$) is stable and the other one ξ_u ($\xi_u \gg r$) is unstable. The rest configuration of the dislocation loop in the presence of a uniform impurity distribution is, thus, given by $\xi(y,t) = \xi_s$. Eq. (5.3) provides a more

realistic estimate for σ_B than reported in Section 2. The condition (5.3) is required to maintain the metastable nature of the system. As a matter of fact, thermal depinning is the mechanism which allows the string to jump out of the pinned configuration ξ_s into the unpinned configuration $\xi = \infty$.

Eq. (5.1) admits of another stationary solution $\xi_n(y)$ with boundary conditions $\xi_n(y) \to \xi_s$ as $y \to \pm\infty$. Such a solution is a critical nucleus which acts just as a saddle-point configuration in the relevant nucleation process [26]. If thermal fluctuations feed energy onto the string up to the ξ_n configuration, then, the nucleus walls can be pulled apart by the constant stress σ. Such a mechanism for the string to overcome the potential barrier that confines it at around ξ_s, requires only a finite activation energy [22, 23]

$$U_n(\sigma) = (8C)^{1/2} \int_{\xi_s}^{\xi_n(y)} \left[\frac{U_n(\xi)}{L_P} - b\sigma\xi - \frac{U(\xi_s)}{L_P} \right]^{1/2} dy . \tag{5.4}$$

The analytical expression for $\xi_n(y)$ depends on the choice of the potential $U(\xi)$ and is generally unknown. To a very rough approximation $\xi_n(y)$ can be envisaged as a square tooth with characteristic length $2y_n$.

The thermal depinning rate μ can be calculated in terms of the quantities y_n and U_n. The rate μ is a typical Arrhenius rate

$$\mu = \nu \exp\left(-\frac{U_n(\sigma)}{kT} \right), \tag{5.5}$$

where the effective "attack frequency" ν is a complicated function of y_n, U_n and T [26, 27].

On rescaling Eq. (5.1) for the stationary string configurations by posing $\xi \to \frac{\xi}{r}$, $y \to \frac{y}{r}$ and $U(y) \to u(y) = U\left(\frac{y}{r}\right)/U_0 L_P$, that is

$$\frac{\partial^2 \xi}{\partial y^2} - \lambda u'(y) + \frac{b\sigma L_P^2}{Cr} = 0 , \tag{5.6}$$

with $\lambda = \frac{L_P U_0}{Cr^2}$, we can distinguish two limiting cases:

(i) continuous pinning approximation. A loop of length $2L_P$ pinned at fixed points is distorted by an external constant stress into a parabola branch, *e.g.* $\xi = \frac{b\sigma}{2C}(L_P^2 - y^2)$. The stress that causes such a loop, obtained by depinning the string locally from a single pinning point at $y = 0$, to bow a distance of the order r is

$$\sigma_1 = \frac{2Cr}{bL_P^2} \sim \frac{\sigma_B}{\lambda} . \tag{5.7}$$

Now, on assuming that the Cottrell potential $U(\xi)$ has a finite range r it is clear that breakaway from a single pin should be impossible at $\sigma < \sigma_1$ [24]. Hence, contrary to the earlier model proposed by GL, depinning may only occur if the dislocation moves away from a group of pins: the breakaway is a *cooperative* process. Under the restriction $\sigma \ll \sigma_B \ll \sigma_1$ or, equivalently, $\lambda \ll 1$ (*short loops*), y_n and U_n can be obtained formally by integrating Eq. (5.6):

$$y_n = \left(\frac{C}{2}\right)^{1/2} \int_{\xi_s}^{\xi_n(y)} \left[\frac{U_n(\xi)}{L_P} - b\sigma\xi - \frac{U(\xi_s)}{L_P}\right]^{-1/2} dy\,, \tag{5.8}$$

while U_n is given in Eq. (5.4). Approximate expressions for y_n and U_n are given in Ref. [24]:

$$y_n = \frac{1}{b\sigma}\left(\frac{2CU_0}{L_P}\right)^{1/2}, \quad U_n = \frac{2}{3}(2y_n)U_0\,. \tag{5.9}$$

(ii) single-pin approximation. The single-pin mechanism outlined in Section 2 gets more and more accurate as σ increases above σ_1 and approaches σ_B. Therefore, the single-pin approximation gives a reasonably good estimate for $U_n(\sigma)$ in the range $[\sigma_1, \sigma_B]$. Furthermore, it should be noticed that the critical nucleus overlaps several pinning-points for $\sigma < \frac{\sigma_B}{\lambda^{1/2}}$, as one sees by equating y_n in Eq. (5.9) to L_P. This remark is consistent with the approximations in *(i)* for $\lambda \ll 1$. In the limit of *long loops* ($\lambda \gg 1$), instead, this suggests us to restrict ourselves to stress value $\frac{\sigma_B}{\lambda^{1/2}} \ll \sigma \ll \sigma_B$, whereas the reader is referred to the original work on the subject [24] for a more exhaustive treatment. The string segment undergoes a *parallel* librational movement in the effective binding potential made up of the Cottrell potential and the tilting term due to the applied stress. Since the latter term is depressed with respect to the former one by the small coupling factor $1/\lambda$, one guesses immediately that

$$y_n \sim L_P\,, \quad U_n \sim U_0\,. \tag{5.10}$$

This guess is confirmed by the analytical calculations of Refs [23] and [24] and supports the earliest formulation of the GL model in Section 2.

The conclusion of both the present and the foregoing Sections is that the dislocation breakaway stress σ_C in the presence of impurity diffusion alone is given in Eq. (3.10) and should be compared with σ_1 in Eq. (5.7). A detailed analysis of the depinning mechanism in the (σ, T) plane is expounded in Ref. [24]. The ratio of the pinned to the depinned dislocation loops varies

widely in the different regions of the (σ, T) plane, the results of Section 4 (no thermal depinning) and 5 (no impurity diffusion) being tenable for suitably small values of T and σ, respectively. However, no matter what (σ, T) plane region, the decrement function $\Delta(\omega)$ at small applied stress values retains its resonant behaviour, *i.e.* $\Delta(\omega) \sim \omega$ as $\omega \to 0$.

On passing we derive what experimentalists call the T-dependence of σ_B. When σ approaches σ_B with $\sigma_B \ll \sigma_C$ (or, equivalently, when neglecting impurity diffusion), the approximate expressions for $U_n(\sigma)$, (5.9) and (5.10), are not valid any more. After expanding the effective binding potential at around the barrier, straightforward algebraic manipulations of the integral (5.4) for $\sigma \sim \sigma_B$ lead to [24]

$$U_n \sim U_0 \left(1 - \frac{\sigma}{\sigma_B}\right)^{5/4} \qquad (\lambda \ll 1) \tag{5.11}$$

and

$$U_n \sim U_0 \left(1 - \frac{\sigma}{\sigma_B}\right)^{3/2} \qquad (\lambda \gg 1). \tag{5.12}$$

Substituting Eqs (5.11) and (5.12) into Eq. (5.5) and solving with respect to σ yield

$$\sigma_B(T) = \sigma_B \left[1 - c_\alpha \left(\frac{kT}{U_0} \ln \frac{\nu}{\mu}\right)^\alpha\right], \tag{5.13}$$

with $\alpha = 4/5$ for $\lambda \ll 1$, $\alpha = 2/3$ for $\lambda \gg 1$, c_α a constant of the order unity and ν the T-dependent attack frequency of Eq. (5.5). The stress $\sigma_B(T)$ is the effective breakaway stress at finite temperature reported in the literature [1]. The calculation of $\sigma_B(T)$ for the case $\sigma_C \ll \sigma_B$ is much more complicated. As suggested by a wealth of measurements on different materials [1], $\sigma_B(T)$ is expected to decrease anyway with increasing the temperature (by a factor up to 50% for T from 0 to 600 K).

6. Nonlinear effects

In the foregoing Sections we assumed that the pinning-points are all distributed along the straight segments connecting the network nodes by the pair: a single network loop gets pinned by the impurities lying nearest to the relevant such a segment and, ultimately, lines them up onto it. This mechanism is tenable only when the impurity density is very low. In the opposite limit the dislocation line cannot be represented by a sequence of pinned vibrating string segments. A sounder picture is provided by a string $\xi(y, t)$ moving in a random background potential (see Fig. 3). Such a potential originates from the overlap of the Cottrell potentials attached to the individual impurities. On assuming for simplicity a high and homogeneous

Fig. 3. Example of weakly pinned dislocation loop. Pinners are represented by circles.

pin distribution on the slip plane, the statistics of the random force exerted on the string becomes Gaussian and almost delta-correlated (*weak pinning*). The latter property is justified when the average inter-impurity distance is much smaller than L_N. The combined action of the background potential and thermal fluctuations is, thus, represented by a Gaussian random force $\eta(y, t)$ with zero mean and auto-correlation function

$$\langle \eta(y,t)\eta(0,0)\rangle = 2D_\eta \delta(y)\delta(t)\,. \tag{6.1}$$

The noise intensity D_η depends on both the temperature and the impurity density of the material under study.

In the presence of an applied stress $\sigma(t)$ directed, for instance, perpendicular to the y-axis like in Fig. 3, the bias exerted on the string is

$$b\sigma\cos\alpha = b\sigma\left[1+\left(\frac{\partial\xi}{\partial y}\right)^2\right]^{-1/2} \simeq b\sigma\left[1-\frac{1}{2}\left(\frac{\partial\xi}{\partial y}\right)^2+\ldots\right]. \tag{6.2}$$

Indeed, since each element of the string is locally pinned, the stress component tangent to $\xi(y,t)$ is ineffective, that is, the relevant bias is compensated by the pinning force. Eq. (6.2) brings in a *nonlinear* term in the corresponding equation of motion for an overdamped dislocation line,

$$B\frac{\partial\xi}{\partial t} - C\frac{\partial^2\xi}{\partial y^2} + \frac{b\sigma(t)}{2}\left(\frac{\partial\xi}{\partial y}\right)^2 = b\sigma(t)+\eta(y,t)\,. \tag{6.3}$$

Eq. (6.3) coincides formally with the Kardar–Parisi–Zhang (KPZ) equation for the growth of interface profiles [28]. The main feature of the KPZ model is the appearance of very large fluctuations (*anomalous diffusion* [29]) as an effect of the nonlinear self-coupling term. In particular, by means of renormalization group techniques one obtains

$$\lim_{t\to\infty}\left\langle \frac{\partial\xi}{\partial y}(y,t)\frac{\partial\xi}{\partial y}(y,t)\right\rangle \sim t^{4/3}\,. \tag{6.4}$$

The exponent 4/3 of the power-law (6.4) is in excess of 1, the exponent of the Einstein diffusion law.

In order to estimate the effects of such large fluctuations on the decrement function at zero frequency, we assume that ω is so small that $\sigma(t)$ can be taken constant over the time interval required for the anomalous diffusion to set in. The corresponding constant bias in Eq. (6.3) produces a shift of the string parallel to itself and can be taken care of by a suitable Galilean transformation. We are thus left with the task of calculating the *excess noise* [29] for the diffusing string in the presence of a constant bias. In the present dislocation, model dissipation is a local process and should be computed for each infinitesimal element of the vibrating string $\frac{\partial \xi}{\partial y} dy$. From Eq. (6.4) it follows immediately that the power-spectrum of $\frac{\partial}{\partial t}\left(\frac{\partial \xi}{\partial y}\right)$ in the regime of anomalous diffusion decays according to the power-law $\omega^{-1/3}$. This is the excess noise law for our driven dislocation line subject to weak pinning. The ω-dependence of $\Delta_R(\omega)$ for $\omega \to 0$ is obtained by multiplying the excess-noise power-law times the linear contribution of the resonance loss at low frequency, *i.e.*

$$\lim_{\omega \to 0} \Delta_R(\omega) \sim \omega \frac{1}{\omega^{1/3}} = \omega^{2/3} . \tag{6.5}$$

The main conclusion of the present Section is that nonlinear effects play an important role at low frequencies. Even if this is not enough to sort out the puzzle of the finite resonance decrement at zero frequency, the law in Eq. (6.5) seems to come much closer to the experimental observations than the GL model: due to nonlinearity, $\Delta_R(\omega)$ decreases with ω slower over the entire frequency range spanned by measurements [4, 8] than predicted by the linear models. Unfortunately, we would obtain a finite value for $\Delta_R(0)$ in Eq. (6.5), only by replacing the exponent 4/3 in Eq. (6.4) with 2 (*ballistic diffusion*). However, in such a case the whole procedure outlined here would be not tenable any longer, being the ballistic diffusion accounted for by merely rescaling the (almost) constant translation speed of the string.

7. Lattice interactions

As early as 1954 Bordoni [30, 31] discovered that the decrement function of certain materials show a maximum on varying the temperature at a fixed forcing frequency. Seeger and Schiller [32] proposed that the Bordoni peak is caused by a thermally activated relaxation process involving dislocations in their slip plane. Indeed, the energy per unit of length of a dislocation, which lies parallel to one of the close-packed directions of the lattice, is a periodic function of its position

$$U_P(\xi) = -\frac{ab\sigma_P}{2\pi} \cos \frac{2\pi}{a} \xi , \tag{7.1}$$

where a is the lattice spacing and σ_P is the Peierls stress. *i.e.* the stress per unit of dislocation length needed to overcome a Peierls potential valley (7.1) without the aid of thermal fluctuations. At finite temperature, however, a dislocation line lying in one Peierls valley can pass over into an adjacent valley even for $\sigma \ll \sigma_P$. The thermal activation mechanism involved is very much the same nucleation mechanism described in Section 5.

The equation of motion for an overdamped string subject to the Peierls potential (7.1) reads

$$B\frac{\partial \xi}{\partial t} - C\frac{\partial^2 \xi}{\partial y^2} = b\sigma - \sigma_P b \sin\frac{2\pi}{a}\xi + \eta(y,t)\,, \tag{7.2}$$

where notation is as in Section 5. On noting that Eq. (7.2) is a perturbed sine-Gordon (SG) equation, the formalism of Refs [26] and [27] applies immediately. A dislocation line thrown across N_P+1 Peierls valleys is made of N_P+1 straight segments resting at the bottom of the potential troughs and N_P short domain walls which bridge two adjacent segments (Fig. 4). The width of such walls is of the order $w(a) = (aC/2\pi\sigma_P b)^{1/2}$ and their rest energy follows from the unperturbed SG equation (7.2) with $A = \sigma = T = 0$, *i.e.* $E_P = CM_P = 2a(2ab\sigma_P C/\pi^3)^{1/2}$. The applied stress σ exerts a pulling force on the walls to the right or to the left in such a way that the string slips in the direction of the stress itself. We agree to call kinks the walls moving to the left and antikinks the walls moving to the right. If the total number of kinks and antikinks $N = N_K + N_{\bar{K}}$ in a dislocation length is small, *i.e.* $L/N \gg w$, a dislocation line obeying the perturbed SG equation (7.2) is approximated to a linear superposition of kinks and antikinks (*dilute gas approximation*).

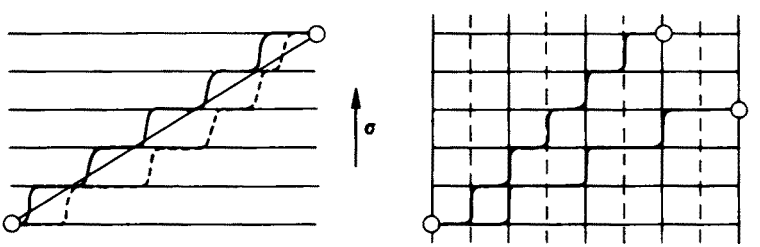

Fig. 4. Example of a dislocation line in the presence lattice potential. Horizontal lines: Peierls valleys; vertical lines: Schottky valleys; solid and dashed curves represent the dislocation line under increasing stress.

At low applied stress the dislocation line can move by two mechanisms:

(i) pair nucleation. This mechanism dominates when the dislocation line runs parallel to the Peierls valleys and has been invoked by Seeger

to explain the appearance of the Bordoni peak. Thermal nucleation of kink-antikink pairs is also responsible for the thermalization of the dislocation line towards a configuration characterized by N_K kinks and $N_{\bar{K}}$-antikinks such that $|N_K - N_{\bar{K}}| = N_P$, the number of so-called geometric kinks (antikinks) and $N_K + N_{\bar{K}} - N_P = 2Ln_0(T)$ where

$$n_0(T) = \left(\frac{2}{\pi}\right)^{1/2} \frac{1}{w} \frac{E_P}{kT} \exp\left(\frac{E_P}{kT}\right), \tag{7.3}$$

is the kink (antikink) density at thermal equilibrium. The parameters U_n and y_n of Section 5 can be calculated exactly for the SG string. The nucleation rate of kink-antikink pairs μ_K is, thus, determined analytically for the whole intensity range of the applied stress. Since we do not make use of such a quantity in the following, we refer the interested reader to Refs [26] and [27] for the relevant analytical expressions.

(ii) kink-antikink diffusion. Sidewise movements of the N_P kinks (antikinks) — we neglect for simplicity the thermal pairs with density (7.3) — are caused by both the applied stress and the thermal noise $\eta(y,t)$. It has been shown that in the dilute gas approximation ($kT \ll E_P$) kinks (antikinks) can be treated like non-interacting quasi-particles with rest mass M_P and radius w. The single kink (antikink) dynamics is described by the Langevin equation

$$\dot{u} = -\gamma u \pm \frac{2\pi}{E_P} F + \eta(t), \tag{7.4}$$

where $u(t)$ denotes the speed of the kink (antikink) center of mass, $\gamma = B$ is the viscosity coefficient, $F = ab\sigma/2\pi$ is the magnitude of the bias exerted by the stress σ upon a quasiparticle and $\pm$ refers to kinks and antikinks, respectively. The random force $\eta(t)$ is a zero mean-valued Gaussian noise with auto-correlation function $\langle \eta(t)\eta(0)\rangle = (2\gamma kT/E_P)\delta(t)$. The stochastic kink (antikink) speed admits of finite mean value $u_F = \pm 2\pi F/\gamma E_P$ and variance kT/E_P.

We calculate now the decrement function in the presence of lattice interactions. The analytical approach of GL is not viable here due to the nonlinearity of the Peierls potential. An alternative approach is due to Seeger and Schiller [32]. These authors replace the vibrating string of the GL model with a chain of interacting quasi-particles, say kinks as shown in Fig. 4 (*kink model*). It is well-known from the analytical solution of the unperturbed SG equation that a kink passes through an antikink, but is reflected by the another kink, and *vice versa*. The relevant interaction potentials are short ranged. Typically, the repulsive kink-kink potential $U_K(s)$ decays like $Ca^2/2s$ at short relative distance s, *i.e.* for $s \leq w$. If we assume

that a dislocation loop L is pinned between two points separated by N_P Peierls valleys as in Fig. 4(a), the N_P geometric kinks repel each other until they achieve an uniform distribution with spacing $s_0 = L/N_P$. The orientation of the dislocation line with respect to the Peierls valleys is given by the angle ϕ, $\sin\phi = a/s_0$. Let us denote the position of the i-th kink by y_i. The equation of motion for the N_P kinks in the small oscillations limit is

$$E_P\ddot{y}_i + \gamma E_P\dot{y}_i = ab\sigma(t) + 2\kappa_K(y_{i-1} - 2y_i + y_{i+1})\,. \tag{7.5}$$

The elastic constant κ_K has been derived from $U_K(s)$, $\kappa_K = Ca^2/2s_0^3$, and the random force $\eta(t)$ neglected compared to the sinusoidal bias due to $\sigma(t) = \sigma_0 e^{i\omega t}$. The calculation of $\Delta_R(\omega)$ for the system (7.5) is now trivial. At low frequencies [32]

$$\Delta_R(\omega) \sim \frac{\pi^5}{960}\Delta_0 \frac{\Lambda(l,\phi)}{\sin\phi}\frac{d}{\omega_0}\frac{\omega}{\omega_0}\,, \tag{7.6}$$

where $\Lambda(l,\phi)$ is the total length per unit of the volume of the dislocation loops with length l and orientation ϕ. Taking the average over ϕ yields the string model result (2.5) for the resonant loss a part from a multiplicative factor of order unity.

The linear kink model (7.5) should be taken with some caution (for a detailed discussion of its equivalence with the string model see Section VIB of Ref. [32]). Since $U_K(s)$ is a short range potential, $U_K(s) \sim \exp(-s/w)$ for $s > w$, a finite value for κ_K exists only if $\sin\phi > a/w(a)$. On passing, we remark that the condition that the dislocation loop is pinned down at the end points requires that $N_P|dU_K/ds| < ab\sigma_B/2\pi$, whence

$$N_P < \frac{ab}{\pi C}\frac{\sigma_B}{\sin^2\phi}\,. \tag{7.7}$$

In the opposite limit $\sin\phi \ll 1$ Seeger and Schiller prediction for $\Delta_R(\omega)$, Eq. (7.6), does not apply. The geometric kinks distributed along the dislocation line undergo a Brownian motion of the type described by the Langevin equation (7.4) and interact with one another elastically. Moreover, nucleation of thermal pairs with density (7.3) introduces nonlinear corrections to the single kink (antikink) dynamics. Not surprisingly, the phenomenon of anomalous diffusion has been observed in the kink model, as well. The $y_i(t)$ autocorrelation functions grow with time according to a power-law with exponent $^4/_3$, thus producing the same excess noise in the string model (6.3). (For details see Ref. [27] and references therein.) Therefore, the conclusions of Section 6 about the effects of nonlinearity, see Eq. (6.5), hold good also when the lattice interactions are included: The kink model cannot account for finite values of $\Delta_R(0)$.

A further complication which might restrict the validity of the kink model arises when one tries to include the lattice substrate interactions. As shown by Schottky [33] this breaches the translational invariance of the kink (antikink) solution, due the appearance of shallow potential valleys (Schottky valleys) which intersect the Peierls valleys (Fig. 4). On assuming that the two families of valleys are orthogonal and applying the technique developed in Ref. [34], we obtain the relevant Langevin equation for a single kink (antikink)

$$\ddot{y} = -\gamma\dot{y} \pm \frac{2\pi}{E_P}F - \frac{2\pi}{E_P}F_S \sin\left(\frac{2\pi}{a'}y\right) , \tag{7.8}$$

where $y(t)$ is the coordinate of the quasi-particle center of mass, a' is the substrate spacing, $F_S = a'b\sigma_S/2\pi ch(\pi^2 w/a')$ and σ_s denotes the Schottky stress, *i.e.* the stress required for a dislocation line of unity length to overcome a Schottky barrier at zero temperature. It should be noticed that the result in Eq. (7.8) is valid for $\sigma_S \ll \sigma_P$, only. For the sake of comparison we remember that the typical values of σ_P in fcc metal lattices range between 10^{-5} to 10^{-3}G, whereas the corresponding values of σ_S are smaller by a factor of the order 10^2 or larger. Note that for such materials σ_S may be bigger that the breakaway stress σ_B by one or two orders of magnitude.

The presence of Schottky potential barriers in Eq. (7.8) posses an important restriction on the number of Peierls valleys that a string of length L can cross. On increasing N_P the inter-kink spacing s_0 may decrease to values smaller than a'. This process takes place by rearranging the geometric kinks to form incommensurate spatial patterns, which resemble themselves a kink structure of the Schottky potential (super-kinks). A fraction ΔN of kinks is, thus, forced to reside at the top of Schottky barriers and, as a result, an internal stress is exerted on the pinning-points. On comparing such an internal stress with the breakaway stress one concludes that the pinning condition requires

$$\Delta N < \frac{a}{a'}\frac{\sigma_B}{\sigma_S}N_P . \tag{7.9}$$

Finally, we comment on the relevance of the lattice interactions at high temperature. The Peierls temperature Θ_P is defined as

$$k\Theta_P = \hbar\omega_P \tag{7.10}$$

with $\omega_P^2 = 2\pi b\sigma_P/aA$ — see Eq. (7.1). In the overdamped regime $\omega_0/d \gg 1$ adopted throughout this Section, the string dynamics becomes purely diffusive at temperatures much larger than $\Theta_P(\omega_P/d)$ as well-known from the

theory of dissipative quantum tunnelling [35]. In most experimental measurements [1] such a condition is not fulfilled and lattice interactions do play a relevant role.

8. Conclusions

The vibrating string model proved successful in interpreting, at least qualitatively, a great deal of experimental data and observation on sound attenuation. Its refinements to include impurity diffusion and lattice interactions (the kink model) provide a reasonable picture of dislocation dynamics in quasi-pure metals. However, a few conceptual difficulties have been pointed out, which might be at the basis of its failure to explain the measured residual friction at low frequency.

First of all, the drag force exerted on the vibrating string by the lattice environment has been *assumed* to be a viscous friction with coefficient $B(T)$. Such an assumption is questionable, indeed. Contributions to the friction force on the dislocation line are of two types:

(i) the phonon bath. The forced string dissipates mechanical energy by radiating elastic waves (or phonons) which propagates through the lattice. As a matter of fact, in the immediate vicinity of the dislocation core the elastic strain is too large for the linear theory of elasticity to apply. This means that phonons can be scattered, absorbed or radiated by the dislocation. The coupling of dislocation with the phonon bath is even stronger on the nonlinear branches of the string (namely, the kinks and antikinks bridging Peierls valleys). The effective damping exerted by an equilibrium phonon bath at temperature T on a kink is proportional to $(kT)^2$ [36];

(ii) nonlinear dynamics. When an unperturbed kink overcomes an obstacle, like a Schottky barrier or a lattice defect, it gets accelerated and, therefore, radiates elastic waves. The intensity of the radiative emission is a function of both the activation energy and the kink velocity. This and other nonlinear mechanisms are operative even at zero temperature. In the absence of detailed quantitative predictions it is hard to assess the relative weight of contributions *(i)* and *(ii)* to the drag force on dislocations. Certainly, the viscous term in Eq. (2.2a) should be replaced with a more complicated functional form $B[\xi]$ of the string $\xi(y,t)$ [36]. The separation of the dislocation dynamics on one side, and the (unperturbed) crystal dynamics on the other, is a very difficult task and its feasibility is far from being proved.

Secondly, the nature and the distribution of the defects in the crystal may endanger the picture of Section 4. In a real sample there may exist different kinds of defects. Considering many mobile pinners on a line together

with several immobile pinners, one finds clusters of them everywhere along the line which grow and decay, disappear completely and appear again at different positions. Moreover, a detailed balance of the pinner exchange between the dislocation core and the Cottrell atmosphere is needed to account for impurity diffusion consistently with a general thermodynamical approach. New arriving pinners are randomly distributed along the network loops, Eq. (3.4), whereas the already existing pinning-points are likely to be thermalized according to the correlated distribution (3.6). *Thermal hysteresis* effects would ensue as a result in both cases.

Finally, we calculated $\Delta_R(\omega)$ by assuming that the depinning events are uncorrelated (apart from the energy conservation requirement), whence the statistical mechanical approach of Section 4. In a recent paper [37] we argued that a stick-and-slip mechanism would be more appropriate to describe the pinning-depinning phenomenon in a dislocation network. A model of self-organized criticality has been proposed which allowed us to calculate $\Delta(0)$ at low stress amplitudes. The very same idea could be generalized to account for another effect which went overlooked in Section 4. The pinner sitting on a dislocation line do diffuse in a random potential due to the action of thermal fluctuations and the dislocation line tension, but also interact with one another. We believe that a stick-and-slip picture of the impurity diffusion process or, alternatively, anomalous impurity diffusion (Section 6) should not be discarded *a priori*. This question is matter of ongoing research work.

This work has been supported by the Istituto Nazionale di Fisica Nucleare (INFN) under the VIRGO project. The project leaders A. Giazotto and A. Brillet are thanked for their assistance and encouragement.

REFERENCES

[1] A.S. Nowick, B.S. Berry, *Anelastic Relaxation in Crystalline Solids*, Academic Press, New York 1972; D.A. Wigley, *Mechanical Properties of Materials at Low Temperature* , Plenum Press, New York 1971.

[2] for review see *e.g.* J. Friedel, *Dislocations*, Pergamon Press, Oxford 1964.

[3] V.B. Braginsky, V.P. Mitrofanov, *Systems with Small Dissipation*, UCP, Chicago 1985.

[4] T.J. Quinn, C.C. Speak, L.M. Brown, *Phil. Mag.* **A65**, 261 (1991).

[5] P.R. Saulson, *Phys. Rev.* **D42**, 2437 (1990).

[6] A. Giazotto, *Phys. Rep.* **C182**, 365 (1989).

[7] A.V. Granato, K. Lücke, in *Physical Acoustics*, W.P. Mason, R.N. Thurston, eds., Vol. IVA, Academic Press, New York 1966, p. 225.

[8] W.P. Mason, in *Physical Acoustics*, W.P. Mason, R.N. Thurston, eds., Vol. VIII, Academic Press, New York 1964, p. 345.

[9] T.A. Read, *Phys. Rev.* **58**, 371 (9140).
[10] T.A. Read, *Trans. A.I.M.E.* **143**, 30 (1941).
[11] A.V. Granato, K. Lücke, *J. Appl. Phys.* **27**, 583 (1956) and **27**, 789 (1956).
[12] J.L. Routbort, H.S. Sack, *J. Appl. Phys.* **37**, 4803 (1966).
[13] U.V. Kocks, *Phil. Mag.* **13**, 541 (1966).
[14] A.J.E. Foreman, M.J. Makin, *Phil. Mag.* **14**, 911 (1966).
[15] J.S. Koehler, in *Imperfections in Nearly Perfect Crystals* Shockley *et al.*, eds., Wiley, New York 1952, p. 197.
[16] G. de Wit, J.S. Koehler, *Phys. Rev.* **116**, 1113 (1959).
[17] G. Leibfried, Oak Ridge Nat. Lab. Progr. Rep. ORNL 2829, 1990; *Dislocations and Mechanical Properties of Crystals*, Wiley, New York 1957.
[18] J. Weertman, J.S. Koehler, *J. Appl. Phys.* **26**, 1190 (1953).
[19] C.L. Bauer, *Phil. Mag.* **11**, 827 (1965).
[20] G. Alefeld, *Phil. Mag.* **11**, 809 (1965).
[21] K. Yamafuji, C.L. Bauer, *J. Appl. Phys.* **36**, 3288 (1966).
[22] for e review see H. Risken, *The Fokker-Planck Equation*, Springer Verlag, Berlin 1984, ch. 5.
[23] L.J. Teutonico, A.V. Granato, K. Lücke, *J. Appl. Phys.* **35**, 220 (1964).
[24] D.G. Blair, T.S. Hutchison, D.N. Rogers, *J. Appl. Phys.* **40**, 97 (1969); *Can. J. Phys.* **49**, 633 (1971).
[25] B.D. Trott, H.K. Birnbaum, *J. Appl. Phys.* **41**, 4418 (1970).
[26] P. Hänggi, F. Marchesoni, P. Sodano, *Phys. Rev. Lett.* **60**, 2563 (1988).
[27] F. Marchesoni, *Acta Phys. Pol.* **B23**, 29 (1992); *Ber. Bunsenges. Phys. Chem.* **95**, 353 (1991).
[28] M. Kardar, G. Parisi, Y.C. Zhang, *Phys. Rev. Lett.* **56**, 889 (1986).
[29] H. van Beijren, R. Kutner, H. Spohn, *Phys. Rev. Lett.* **54**, 2026 (1985).
[30] P.G. Bordoni, *J.A.S.A.* **26**, 495 (1954).
[31] for review see *e.g.* D.H. Niblett, in *Physical Acoustics*, W.P. Mason, R.N. Thurston, eds., Vol. IIIA, Academic Press, New York 1966, p. 77.
[32] A. Seeger, P. Schiller, in *Physical Acoustics*, W.P. Mason, R.N. Thurston, eds., Vol. IIIA, Academic Press, New York 1966, p. 361.
[33] G. Schottky, *Phys. Status. Solidi* **5**, 697 (1964).
[34] F. Marchesoni, *Phys. Lett.* **A115**, 29 (1986).
[35] P. Hänggi, P. Talkner, M. Borkovec, *Rev. Mod. Phys.* **62**, 251 (1990).
[36] F. Marchesoni, C.R. Willis, *Europhys. Lett.* **12**, 491 (1990).
[37] G. Cagnoli, L. Gammaitoni, F. Marchesoni, D. Segoloni, submitted to *Phil. Mag.*, 1993.